

Fusion and elastic scattering of ${}^6\text{Li} + {}^{58}\text{Ni}$ at low energies

Elí F. Aguilera^{1,*}, Paulina Amador-Valenzuela¹, Enrique Martínez-Quiroz¹, David Lizcano¹, Araceli García-Flores¹, and James J. Kolata²

¹Departamento de Aceleradores, Instituto Nacional de Investigaciones Nucleares, Apartado Postal 18-1027, Código Postal 11801, México, Distrito Federal, México

²Physics Department, University of Notre Dame, Notre Dame, Indiana, 46556-5670, USA

Abstract. Sub-barrier fusion cross sections (σ_{fus}) for the ${}^6\text{Li} + {}^{58}\text{Ni}$ system, obtained from the respective evaporation protons, are examined in the present work. With respect to expectations of a simple one-dimensional barrier penetration model, a large enhancement of the data is observed. Good consistency with equivalent data reported previously for similar systems is found. A comparison with total reaction cross sections (σ_R), deduced from elastic scattering measurements reported previously, indicates that σ_{fus} is close to σ_R within the measured energy range. To estimate the contribution of complete fusion (CF), an optical model analysis of the elastic scattering data is performed where CF is identified with the absorption in a short range volume potential. A surface polarization potential is added to the bare nuclear potential to simulate the effect of peripheral reactions. The results obtained indicate that other mechanisms different from CF may be dominant, especially in the lower energy region.

1 Introduction

Several measurements have been done lately to study different reactions induced by the stable weakly-bound nucleus ${}^6\text{Li}$ [1–5]. However, the different data sets are still far from being completely understood. An analysis involving the ${}^6\text{Li} + {}^{58}\text{Ni}$ system is presented here.

Total fusion cross sections were recently measured for this system [6], which complement the elastic scattering data previously reported [1]. Evaporated protons were measured to obtain the respective proton cross sections and then statistical model calculations were used to map them into fusion cross sections [6]. The results are shown in figure 1 with red circles. The total reaction cross sections obtained earlier at similar energies for the same system [1], are shown with black squares. The barrier is indicated with the vertical arrow, so these are mostly sub-barrier data. The barrier parameters ($V_B = 12.36$ MeV, $R_B = 9.02$ fm, $\hbar\omega_0 = 3.63$ MeV) were obtained from the Sao Paulo Potential (SPP) [7] and used in the single barrier penetration model (BPM) of Wong [8] to obtain the dashed line. The solid curve is the result of adding a short range imaginary potential to the real SPP and doing optical model calculations. The absorption in such imaginary potential is then identified with complete fusion. Because of the approximations involved in Wong's model, this should be a more realistic BPM prediction. One can see that the data present a big enhancement with respect to this curve. The dotted line is the result of coupled channel calculations including inelastic excitation of the first 2+

and 3- states in ${}^{58}\text{Ni}$. The conclusion is that these inelastic couplings cannot explain the enhancement, i.e., additional channels would be needed in order to describe the data.

Using a well-known prescription to reduce data [9–12] (see axis labels on Fig. 2), a comparison was made in Fig. 2 with data reported for the same projectile and similar-mass targets. The present data are fairly consistent with results for ${}^{59}\text{Co}$ [13], ${}^{64}\text{Ni}$ [14], and ${}^{64}\text{Zn}$ [3], and one can see from figure 2 that the three data sets show a large sub-barrier enhancement with respect to BPM predictions. Therefore, it would seem that the origin for the enhancement can be ascribed to the projectile, independent of the target, although this conclusion is not quite supported by the wide spread of the data at the lower energies. Such spread was ascribed in Ref. [6] to a possible effect of direct reactions, which could be contaminating the fusion data reported for some of the systems. For the case of the ${}^6\text{Li} + {}^{64}\text{Zn}$ system, for instance, it is possible that the data include contributions from one-neutron and/or one-proton transfer reactions [3]. The present data do not include such contributions (protons from neutron stripping were estimated and corrected for by doing appropriate DWBA calculations, while no protons are expected from proton stripping [6]), but could in principle contain contributions from certain direct processes which cannot be distinguished with the experimental technique used. To be more specific, if a deuteron is transferred to the target and the resulting product becomes excited above the proton emission threshold, then some evaporation protons would be emitted in this process which cannot be distinguished from protons coming from fusion. To estimate

*e-mail: eli.aguilera@inin.gob.mx

possible contributions from direct or peripheral processes, a reanalysis of the previous data for elastic scattering was done.

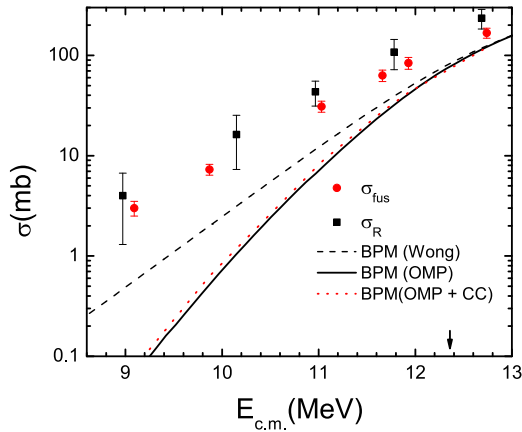


Figure 1. Fusion ([6]) and total reaction ([1]) cross section data for ${}^6\text{Li} + {}^{58}\text{Ni}$. The curves correspond to calculations described in the text. Figure adapted from Ref. [6]

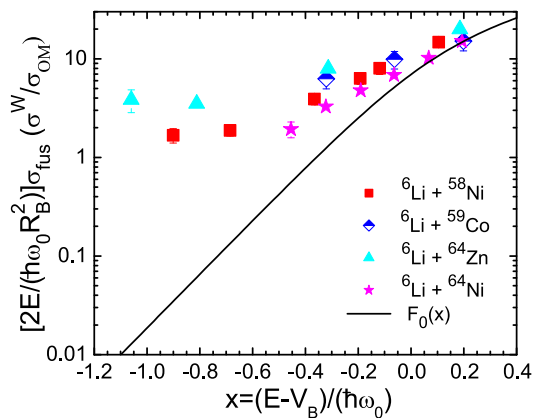


Figure 2. Comparison of reduced cross sections for four systems. The curve represents the Universal Fusion Function, which corresponds to expectations for normal systems. Figure taken from Ref. [6]

2 Analysis of elastic scattering

The five elastic scattering angular distributions for ${}^6\text{Li} + {}^{58}\text{Ni}$ that were published in Ref. [1] were taken to make an optical model analysis. A surface polarization potential was introduced to simulate direct reactions, using in addition the SPP as the bare potential and a short-range imaginary potential ($W_0 = 50$ MeV, $r_0 = 1.0$ fm, $a_0 = 0.1$

fm) to describe fusion. The surface polarization potential was taken to have a derivative Woods-Saxon shape with 4 parameters: the real and imaginary depths (V_S , W_S), one common radius and one common diffuseness. From a first search, we were able to fix the radius at 1.47 fm and the diffuseness at 0.68 fm for all energies, so only the depths V_S , W_S were varied for each energy.

Figure 3 shows the results of the final fits. One can see that a very good description of the data is achieved. Also, the obtained total reaction cross sections were consistent with those reported in the original paper [1], plotted in Fig. 1. Figure 4 shows the values of depths obtained from the fit, as a function of the energy. The black squares are the imaginary depths and the red circles are the real depths. The imaginary depths were approximated by straight line segments, as shown by the black lines, applying then the dispersion relation, given by the following formula:

$$V(E) = V(E_S) + (E - E_S) \frac{1}{\pi} \oint \frac{W(r, E')}{(E' - E_S)(E' - E)} dE'. \quad (1)$$

The result is the red curve, which describes well the red points. So, the real and imaginary polarization potentials satisfy the dispersion relation, as they should.

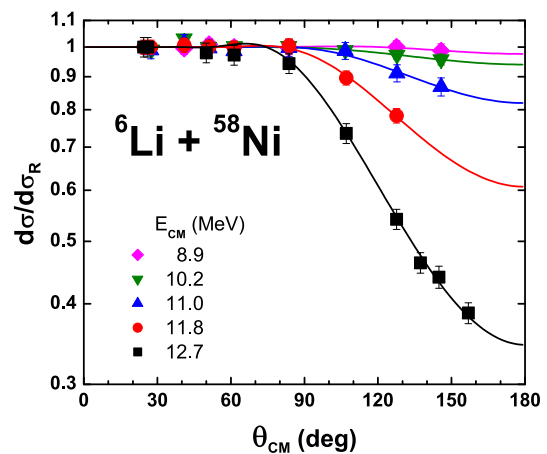


Figure 3. Elastic scattering angular distributions for ${}^6\text{Li} + {}^{58}\text{Ni}$ (symbols), from Ref. [1], and results of the Optical Model fits obtained in the present work (curves).

In this analysis, complete fusion (CF) is identified with the absorption in W_0 , and this absorption is represented in figure 5. The empty circles represent the complete fusion cross sections predicted in this analysis. It is quite surprising because the “experimental” values are much larger, represented by the filled circles. The effect of changing the radius of the surface potential was investigated. When a value of 1.61 fm instead of 1.47 fm was used for that radius, the results are shown by the blue diamonds. There is some sensitivity to the radius, but the changes are small, so there is no real qualitative change. Anyhow, these results

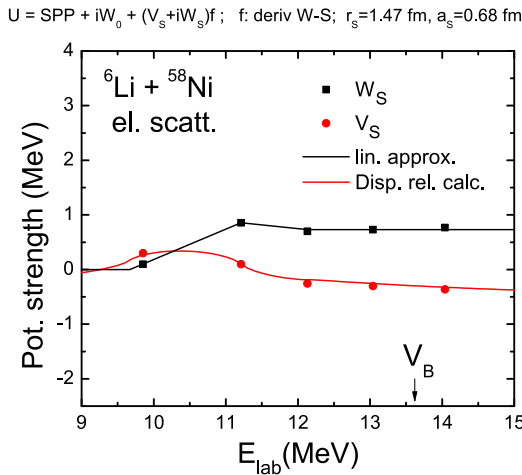


Figure 4. Real (V_S) and imaginary (W_S) potential depths obtained from the fits in Fig. 3

should be considered as preliminary as there might be ambiguities in the potential that still need to be investigated. If the results are confirmed, this would mean that some processes different from CF dominate the data at these low energies. These processes could be incomplete fusion (ICF) or even some of the direct processes mentioned in Section 1. It is worth mentioning that Di Pietro and collaborators arrived at similar conclusions in the case of the ${}^6\text{Li} + {}^{64}\text{Zn}$ data [3]. They showed that their relative populations of heavy residues could not be explained by CF calculations alone but exhibited evidence for an important contribution of ICF and/or Direct Cluster Transfer.

Finally, it may be pointed out that figure 5 is reminiscent of the situation observed for the neutron halo projectile ${}^6\text{He}$. Figure 6 shows a similar plot but for the ${}^6\text{He} + {}^{64}\text{Zn}$ system. In this case also the fusion cross sections are much lower than the total reaction cross sections. Both data sets in figs. 5 and 6 correspond to comparable energy regions in terms of the respective barrier, and there is a remarkable similarity between them. It is possible, therefore, that between the weakly-bound neutron-halo nucleus ${}^6\text{He}$ and the stable weakly-bound isotope ${}^6\text{Li}$ there are more similarities than are usually conceded.

3 Conclusions

Fusion cross sections (σ_{fus}) derived for ${}^6\text{Li} + {}^{58}\text{Ni}$ from measurements of proton evaporation yields are presented. σ_{fus} is seen to be close to σ_R , i.e., fusion appears to be dominant in the respective energy region. A good global consistency is observed with data for the same projectile but targets of ${}^{59}\text{Co}$, ${}^{64}\text{Ni}$, and ${}^{64}\text{Zn}$, but considerable data spread is noted in the lower energy region. A surface polarization potential was introduced which describes well the elastic scattering data for ${}^6\text{Li} + {}^{58}\text{Ni}$ and satisfies the dispersion relation. The respective Optical Model calculation predicts a low contribution of CF to TF, so ICF

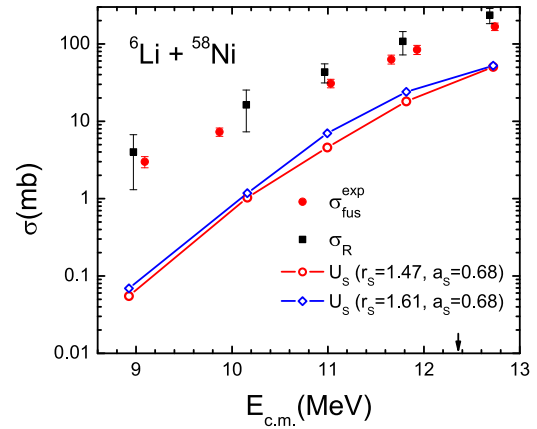


Figure 5. CF cross sections obtained from the present Optical Model analysis corresponding to two different values of r_s , the radius of the surface polarization potential.

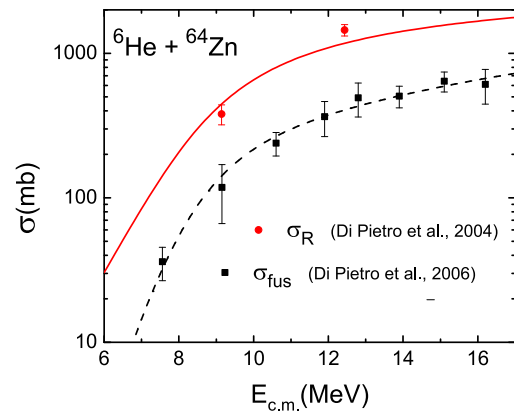


Figure 6. Fusion and total reaction cross sections for ${}^6\text{He} + {}^{64}\text{Zn}$. Data from Refs. [15] and [16], respectively. Figure adapted from Ref. [17].

or other direct (distant) processes would be important. If the above conclusion is confirmed, ${}^6\text{Li}$ could behave more similar to ${}^6\text{He}$ than is usually thought.

4 Acknowledgments

Work partially supported by CONACYT (México) and by NSF (USA) under grant No PHY14-01343.

References

- [1] E. F. Aguilera, E. Martínez-Quiroz, D. Lizcano, A. Gómez-Camacho, J. J. Kolata, L. O. Lamm, V. Guimarães, R. Lichtenthäler, O. Camargo, F. D. Becchetti, H. Jiang, P. A. DeYoung, P. J. Mears, and T. L. Belyaeva, Phys. Rev. C **79**, 021601(R) (2009)

- [2] M. Zadro, *et al.*, Phys. Rev. C **87**, 054606 (2013)
- [3] A. DiPietro, *et al.*, Phys. Rev. C **87**, 064614 (2013)
- [4] D. R. Otomar, *et al.*, Phys. Rev. C **87**, 014615 (2013)
- [5] S. Kalkal, *et al.*, Phys. Rev. C **93**, 044605 (2016)
- [6] E. F. Aguilera, E. Martinez-Quiroz, P. Amador-Valenzuela, D. Lizcano, A. García-Flores, J. J. Kolata, A. Roberts, G. V. Rogachev, G. F. Peaslee, V. Guimarães, F. D. Becchetti, A. Villano, M. Ojaruega, Y. Chen, H. Jiang, M. Febbraro, P. A. DeYoung, and T. L. Belyaeva, Phys. Rev. C **96**, 024616 (2017).
- [7] L. C. Chamon, B. V. Carlson, L. R. Gasques, D. Pereira, C. De Conti, M. A. G. Alvarez, M. S. Hussein, M. A. Cândido Ribeiro, E. S. Rossi, Jr., and C. P. Silva, Phys. Rev. C **66**, 014610 (2002)
- [8] C. Y. Wong, Phys. Rev. Lett. **31**, 766 (1973)
- [9] N. V. S. V. Prasad, A. M. Vinodkumar, A. K. Sinha, K. M. Varier, D. L. Sastry, N. Madhavan, P. Sugathan, D. O. Kataria, and J. J. Das, Nucl. Phys. **A603**, 176 (1996)
- [10] L. R. Gasques, L. C. Chamon, D. Pereira, M. A. G. Alvarez, E. S. Rossi Jr., C. P. Silva, and B. V. Carlson, Phys. Rev. C **69**, 034603 (2004)
- [11] L. F. Canto, P. R. S. Gomes, J. Lubian, L. C. Chamon, and E. Crema, J. Phys. G: Nucl. Part. Phys. **36**, 015109 (2009)
- [12] L. F. Canto, P. R. S. Gomes, J. Lubian, L. C. Chamon, and E. Crema, Nucl. Phys. **A821**, 51 (2009)
- [13] C. Beck, *et al.*, Phys. Rev. C **67**, 054602 (2003).
- [14] M. M. Shaikh, *et al.*, Phys. Rev. C **90**, 024615 (2014)
- [15] A. Di Pietro *et al.*, Phys. At. Nucl. **69**, 1366 (2006)
- [16] A. Di Pietro *et al.*, Phys. Rev. C **69**, 044613 (2004)
- [17] E. F. Aguilera and J. J. Kolata, Phys. Rev. C **85**, 014603 (2012)